

Telomere shortening impairs organ regeneration by inhibiting cell cycle re-entry of a subpopulation of cells

A.Satyanarayana, S.U.Wiemann, J.Buer^{1,2}, J.Lauber², K.E.J.Dittmar², T.Wüstefeld, M.A.Blasco³, M.P.Manns and K.L.Rudolph⁴

Department of Gastroenterology, Hepatology and Endocrinology and ¹Department of Microbiology, Medical School Hannover, Carl-Neuberg-Straße 1, D-30625 Hannover, ²Department of Cell Biology, GBF, Germany and ³Department of Oncology, Canto Blanco, Madrid, Spain

⁴Corresponding author
e-mail: Rudolph.Lenhard@Mh-Hannover.de

Telomere shortening limits the regenerative capacity of primary cells *in vitro* by inducing cellular senescence characterized by a permanent growth arrest of cells with critically short telomeres. To test whether this *in vitro* model of cellular senescence applies to impaired organ regeneration induced by telomere shortening *in vivo*, we monitored liver regeneration after partial hepatectomy in telomerase-deficient mice. Our study shows that telomere shortening is heterogeneous at the cellular level and inhibits a subpopulation of cells with critically short telomeres from entering the cell cycle. This subpopulation of cells with impaired proliferative capacity shows senescence-associated β -galactosidase activity, while organ regeneration is accomplished by cells with sufficient telomere reserves that are capable of additional rounds of cell division. This study provides experimental evidence for the existence of an *in vivo* process of cellular senescence induced by critical telomere shortening that has functional impact on organ regeneration.

Keywords: cell cycle/DNA damage/G₁/S arrest/organ regeneration/senescence

Introduction

Telomeres are specialized nucleoprotein structures at the end of eukaryotic chromosomes (Blackburn, 1991). Loss of telomeric DNA via the end replication problem limits the proliferative capacity of primary cells *in vitro* at the stage of cellular senescence (Harley *et al.*, 1990; Yu *et al.*, 1990; Wright and Shay, 1992; Allsopp *et al.*, 1995). Cells cannot proliferate beyond the senescence checkpoint unless the senescence pathway which is guarded by p53 and Rb is experimentally perturbed (Shay *et al.*, 1991; Bond *et al.*, 1996; Vaziri and Benchimol, 1996; Jarrard *et al.*, 1999; Bringold and Serrano, 2000; Smogorzewska and de Lange, 2002). Experimental proof for the telomere hypothesis of ‘cell aging’ has come from studies showing that the ectopic expression of telomerase immortalizes primary human fibroblasts (Bodnar *et al.*, 1998).

In humans, telomere shortening has been demonstrated in various tissues during aging (Lindsey *et al.*, 1991; Vaziri *et al.*, 1993, 1994; Allsopp *et al.*, 1995; Chang and Harley, 1995) and in chronic diseases of elevated cell turnover (Kitada *et al.*, 1995; Ball *et al.*, 1998; Boulwood *et al.*, 2000; Effros, 2000; Wiemann *et al.*, 2002), and some of the recent studies have reported increased senescence-associated β -galactosidase activity in aged human skin (Dimri *et al.*, 1995) and liver cirrhosis (Paradis *et al.*, 2001; Wiemann *et al.*, 2002). These data have fueled the debate that cellular senescence induced by telomere shortening might impact on regeneration of tissues and organs during aging and chronic high-turnover diseases. Experimental support for the telomere hypothesis of impaired organ regeneration during aging and chronic diseases has come from studies in telomerase-deficient mice (mTERC^{-/-}). Late-generation mTERC^{-/-} mice with critically short telomeres show defects in homeostasis of highly proliferative organs (Lee *et al.*, 1998) and these organ systems are affected by premature aging phenotypes (Herrera *et al.*, 1999; Rudolph *et al.*, 1999). In addition, liver regeneration was impaired in mTERC^{-/-} mice in different model systems of liver regeneration (Rudolph *et al.*, 2000). First, in response to partial hepatectomy (PH), liver mass restoration was delayed and hepatocytes showed signs of telomere dysfunction (anaphase bridges) and a suppressed progression through the G₂/M stage of the cell cycle (Rudolph *et al.*, 2000). Secondly, in a model of acute liver failure, telomere shortening correlated with decreased hepatocyte proliferation and increased hepatocyte apoptosis. Finally, in response to chronic organ damage, the impaired organ regeneration in mTERC^{-/-} mice results in a premature development of progressive disease stages such as liver cirrhosis (Rudolph *et al.*, 2000) and colitis ulcerosa (J.Wedemeyer and K.L.Rudolph, unpublished data)—diseases in humans that are characterized by critical telomere shortening (Kinouchi *et al.*, 1998; Wiemann *et al.*, 2002).

The phenotype of impaired organ regeneration in mTERC^{-/-} mice has been linked to the prevalence of critically short telomeres (Hemann *et al.*, 2001), and the cell cycle inhibitor p53 was identified as mediating the adverse effects of telomere shortening (Chin *et al.*, 1999). A current hypothesis is that critical telomere shortening leads to telomere dysfunction and activates DNA damage responses resulting in cell cycle arrest and/or apoptosis, as has been demonstrated in primary cell lines entering senescence *in vitro*. Since the replicative lifespans of subclones of a given cell line show high variability depending on the initial telomere length of individual subclones prior to expansion, it has been postulated that telomere length at the cellular level determines whether a cell enters senescence or continues to proliferate (Allsopp and Harley, 1995). Our study explores whether this model

applies to the impaired regenerative capacity of organ systems *in vivo* by analyzing the cellular responses to PH in late-generation mTERC^{-/-} mice and mTERC^{+/+} controls. We present direct evidence for induction of cellular senescence by critical telomere shortening at the cellular level *in vivo* and its impact on organ regeneration.

Results

Telomere shortening limits the number of cells participating in organ regeneration

The resting liver is a mitotically inactive organ with over 95% of the cells in the G₀ stage of the cell cycle. In

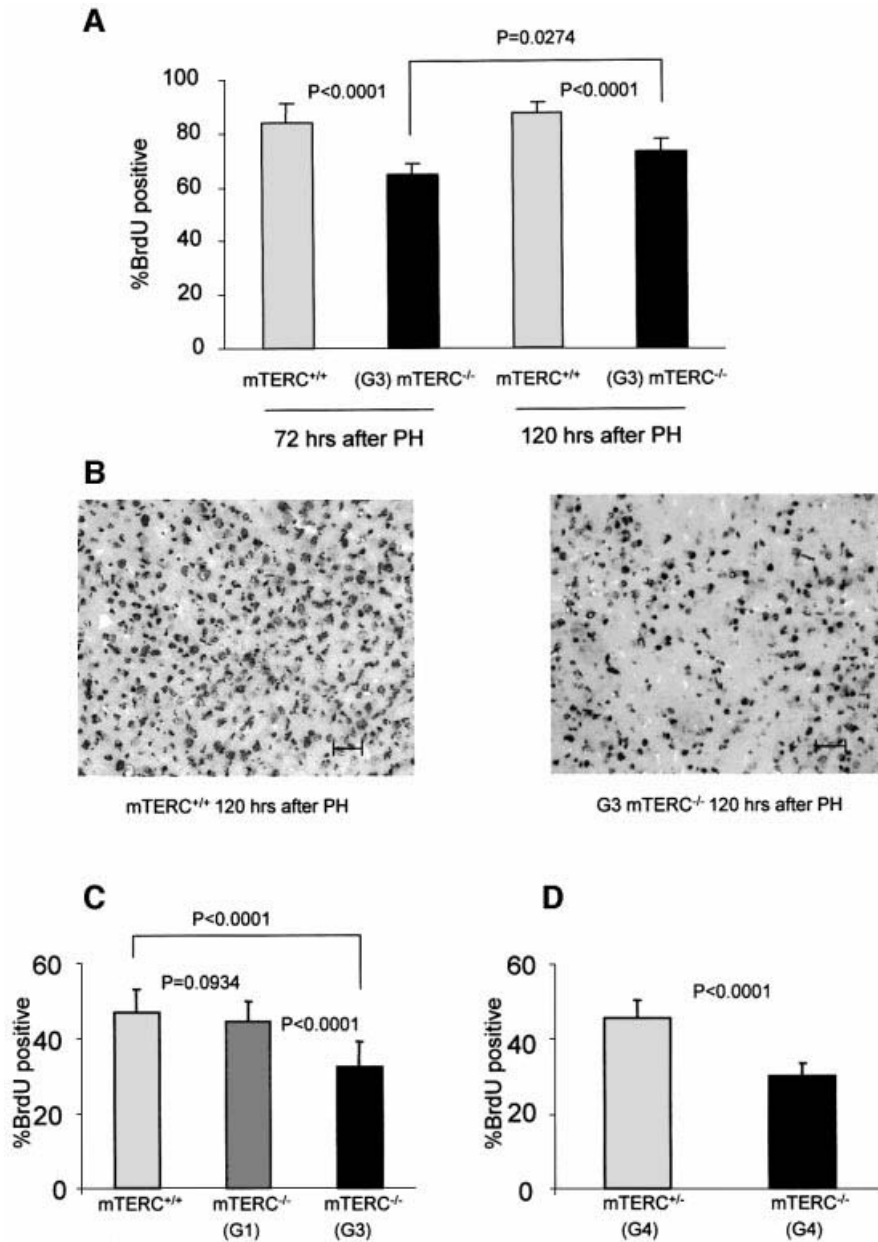


Fig. 1. Telomere shortening inhibits a subpopulation of cells from participating in liver regeneration. The percentage of liver cells incorporating BrdU in response to PH under continuous BrdU labeling is higher in mTERC^{+/+} than in G₃ mTERC^{-/-} mice. (A) Rate of BrdU-labeled liver cells 72 h after PH [83.83 ± 7.44% in mTERC^{+/+} (*n* = 5) versus 64.5 ± 4.28% in G₃ mTERC^{-/-} (*n* = 5), *p* < 0.0001] and 120 h after PH [86.96 ± 4.33 in mTERC^{+/+} (*n* = 5) versus 72.30 ± 5.45% in G₃ mTERC^{-/-} (*n* = 5), *p* < 0.0001]. (B) Representative photographs of BrdU staining pattern in mTERC^{+/+} and G₃ mTERC^{-/-} mice 120 h after PH under continuous BrdU infusion (bar, 150 μm). (C) Percentage of cells incorporating BrdU at the first peak stage of S-phase (48 h after PH) under 2 h of BrdU pulse labeling: 47.03 ± 6.33% in mTERC^{+/+} (*n* = 5) versus 44.45 ± 5.26% G₁ mTERC^{-/-} (*n* = 5, *p* = 0.0934) and 32.31 ± 6.65% G₃ mTERC^{-/-} (*n* = 5, *p* < 0.0001). A significant reduction in the BrdU index is evident in G₃ mTERC^{-/-} mice, whereas G₁ mTERC^{-/-} mice show a similar rate of BrdU-positive liver cells compared with mTERC^{+/+} mice, indicating that telomere length but not lack of telomerase impacts on the number of cells participating in organ regeneration. (D) Percentage of cells incorporating BrdU at the first peak stage of S-phase (48 h after PH) under 2 h of BrdU pulse labeling: 45.52 ± 4.65% in G₄ mTERC^{+/+} (*n* = 5) versus 29.90 ± 3.25% G₄ mTERC^{-/-} (*n* = 5, *p* < 0.0001). G₄ mTERC^{-/-} mice show a rescue in the percentage of BrdU-positive cells, indicating that telomere stabilization by telomerase re-expression rescues suppression of cell cycle re-entry of a subpopulation of cells.

response to PH, liver cells re-enter the cell cycle in a highly synchronized fashion and regenerate lost mass by one to two rounds of replication within a week, thus representing a system in which somatic cell division regenerates organ mass without a direct need for a specific stem cell population (Fausto, 2000; Kountouras *et al.*, 2001). To analyze the impact of telomere shortening on organ regeneration at the cellular level, continuous labeling of all the proliferating cells with 5-bromo-2'-deoxyuridine (BrdU) was performed in G₃ mTERC^{-/-} and mTERC^{+/+} controls until two rounds of replication (120 h after PH) had been completed. After both the first round (72 h after PH) and the second round (120 h after PH) of DNA replication, the number of cells participating in liver regeneration was significantly reduced in G₃ mTERC^{-/-} mice compared with mTERC^{+/+} mice (Figure 1A and B). These data indicated that telomere shortening inhibited a subpopulation of liver cells from participating in organ regeneration.

Previous studies in late-generation mTERC^{-/-} mice have shown that telomere shortening leads to defective regeneration and impaired organ homeostasis (Lee *et al.*, 1998; Herrera *et al.*, 1999; Rudolph *et al.*, 1999, 2000). To test whether inhibited cell cycle entry of a subpopulation of cells in G₃ mTERC^{-/-} mice is due to critical telomere shortening, we monitored liver regeneration in G₁ mTERC^{-/-} mice (i.e. animals lacking telomerase activity but having long telomere reserves) (Blasco *et al.*, 1997). S-phase activity in response to PH peaks at 48 h after surgery. Two hours of pulse labeling with BrdU at this time point revealed similarly high rates of BrdU incorporation in G₁ mTERC^{-/-} and mTERC^{+/+} mice compared with a significantly lower rate in G₃ mTERC^{-/-} mice (Figure 1C). In addition, telomere stabilization by telomerase re-expression in G₄ mTERC^{+/-} mice, derived from a cross of G₃ mTERC^{-/-} mice and mTERC^{+/-} mice (Samper *et al.*, 2001), completely rescued the defective regenerative response following PH, which was present in G₄ mTERC^{-/-} littermates (Figure 1D). Together, these data indicated that the phenotype of a decreased population of cells entering the cell cycle during organ regeneration is due to telomere shortening, independent of telomerase *per se*, but can be rescued by telomere stabilization in mice with critically short telomeres.

Critical telomere shortening at the cellular level blocks cell cycle re-entry of a subpopulation of liver cells in G₃ mTERC^{-/-} mice

A possible explanation for the inhibition of cell cycle re-entry in a subpopulation of cells in G₃ mTERC^{-/-} mice is that telomeres in cells of an organ system are heterogeneous, and that only cells with critically short dysfunctional telomeres are inhibited from entering the cell cycle. To test this hypothesis, telomere length was analyzed at the single-cell level using quantitative fluorescence *in situ* hybridization (qFISH) (Gonzalez-Suarez *et al.*, 2000; Poon and Landsorp, 2001) in combination with BrdU staining (Figure 2A–C). With this approach, it is possible to compare telomere lengths directly between liver cells participating in organ regeneration (BrdU positive) and liver cells inhibited from cell cycle re-entry (BrdU negative). In mTERC^{+/+} mice, BrdU-positive and BrdU-negative liver cells (120 h after PH and continuous

labeling with BrdU) showed similar mean telomere fluorescence intensities (Figure 2D, E and H). As expected, the overall telomere fluorescence intensity is lower in G₃ mTERC^{-/-} mice than in mTERC^{+/+} mice. Interestingly, however, within the liver of G₃ mTERC^{-/-} the telomere fluorescence intensity was significantly weaker in the subpopulation of cells inhibited from cell cycle re-entry (BrdU negative) than in the population of proliferating cells (BrdU positive) (Figure 2F–H). In addition to lower mean telomere fluorescence intensity, the non-proliferating cells also had lower minimum fluorescence intensities compared with the proliferating cells in G₃ mTERC^{-/-} mice (data not shown). The observation that the mean telomere fluorescence intensities between BrdU-positive and BrdU-negative cells 120 h after PH were similar in mTERC^{+/+} mice indicates that BrdU staining and cell cycle stage did not interfere with hybridization and quantification of the telomeric probe at the telomeres. These data gave direct evidence that critically short telomeres at the cellular level limit the proliferative capacity of cells within an organ system.

Non-proliferating cells with critically short telomeres in mTERC^{-/-} are senescent

A possible mechanism for inhibition of cell cycle re-entry in a subpopulation of cells is the induction of cellular senescence, which in primary human cells is induced after 50–70 cell doublings, first affecting subclones with critically short telomeres of a given cell line *in vitro* (Allsopp and Harley, 1995). To test directly whether the non-proliferating cells in G₃ mTERC^{-/-} entered senescence, senescence-associated (SA) β-galactosidase staining (Dimri *et al.*, 1995) was conducted on liver samples 120 h after PH to compare directly the percentage of SA β-galactosidase-positive cells with the percentage of non-proliferating cells (BrdU negative). This method revealed significantly increased rates of senescent cells in G₃ mTERC^{-/-} mice compared with mTERC^{+/+} mice (Figure 3A and B). Even though SA β-galactosidase staining is widely used as a marker of senescence, it has been shown that false-positive results occur *in vitro* in cell cultures exposed to various stresses (Severino *et al.*, 2000). To exclude unspecific non-senescence-related SA β-galactosidase staining, a co-staining combining BrdU staining with SA β-galactosidase staining was conducted. This co-staining revealed a strong coincidence of β-galactosidase activity with non-proliferating cells (BrdU negative) in G₃ mTERC^{-/-} mice. Specifically, only 13 ± 4.84% of the SA β-galactosidase-positive cells were BrdU positive, whereas 79 ± 6.2% of the SA β-galactosidase-negative fraction of cells showed BrdU incorporation (Figure 3C).

To show directly that the SA β-galactosidase-positive cells in G₃ mTERC^{-/-} mice were inhibited from cell cycle re-entry by critically short telomeres, a co-staining combining SA β-galactosidase staining with telomeric qFISH was carried out. As anticipated from the above results, this analysis revealed significantly weaker telomere fluorescence intensities in SA β-galactosidase-positive cells than in SA β-galactosidase-negative cells in G₃ mTERC^{-/-} mice (Figure 3D and E). In contrast, mTERC^{+/+} mice showed no difference in the telomere fluorescence intensity comparing SA β-galactosidase-positive and -negative cells.

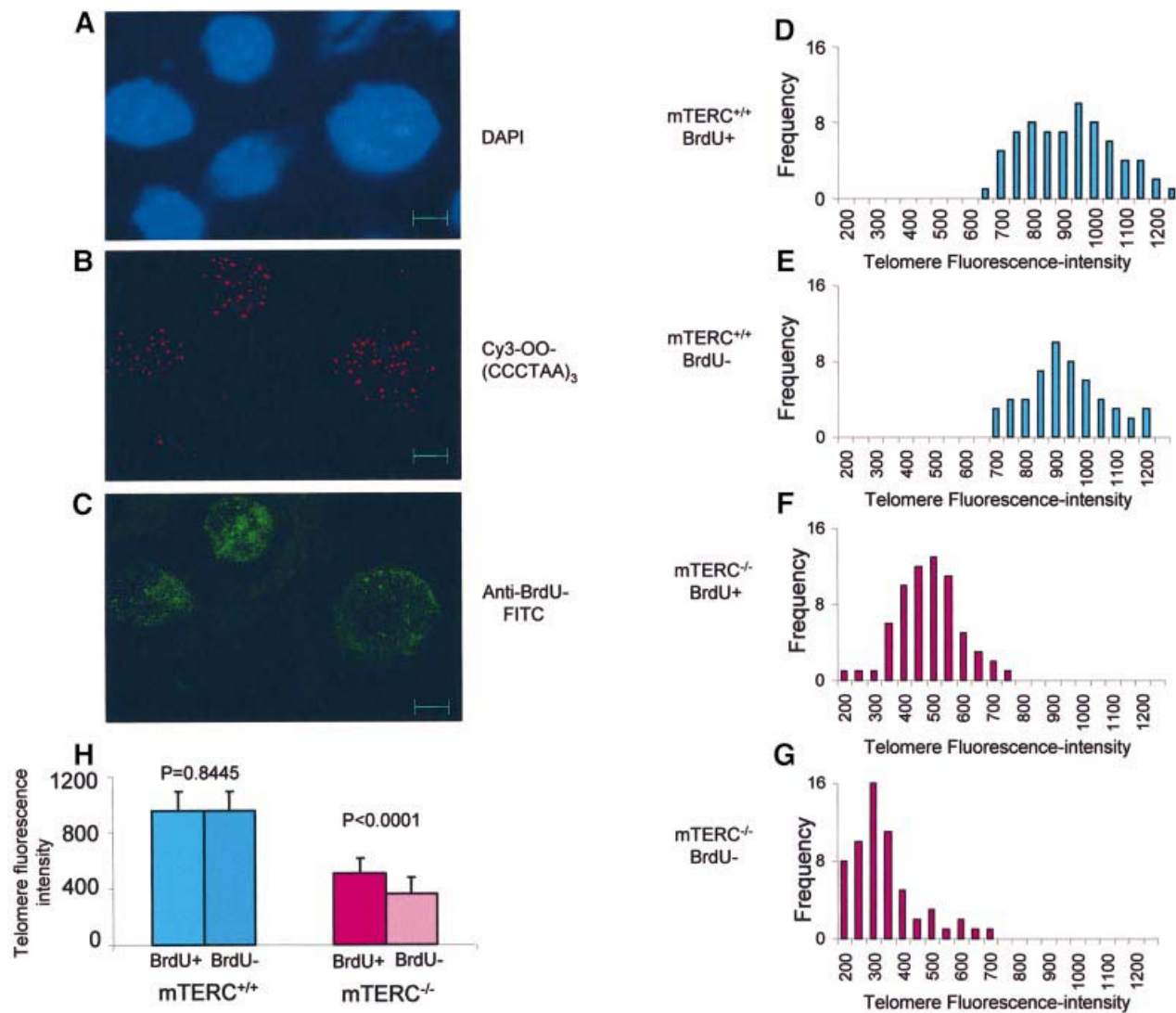


Fig. 2. Critical telomere shortening at the cellular level inhibits cell cycle re-entry of a subpopulation of cells. Telomere length analysis at cellular level by qFISH was combined with BrdU staining (A–C). (A) DAPI counterstaining. (B) qFISH with a telomere-specific probe Cy3-OO-(CCCTAA)₃. (C) BrdU staining with anti-BrdU monoclonal antibody and FITC-conjugated secondary antibody. The liver samples from 120 h of continuous BrdU labeling after PH were used to measure and compare the telomere fluorescence intensities in BrdU-positive and BrdU-negative cells. In total, the fluorescence intensities of telomere spots were analyzed from 69 BrdU-positive and 54 BrdU-negative nuclei from mTERC^{+/+} ($n = 5$), and 66 BrdU-positive and 60 BrdU-negative nuclei from G₃ mTERC^{-/-} ($n = 5$) mice. (D) Telomere fluorescence intensity of BrdU-positive cells in mTERC^{+/+} mice. (E) BrdU-negative cells in mTERC^{+/+} mice. (F) BrdU-positive cells in G₃ mTERC^{-/-} mice. (G) BrdU-negative cells in G₃ mTERC^{-/-} mice. (H) The mean telomere fluorescence intensities of BrdU-positive cells (952.53 ± 144.19) and BrdU-negative cells (957.44 ± 130.57) in mTERC^{+/+} mice, and BrdU-positive cells (509.65 ± 101.30) and BrdU-negative cells (364.94 ± 116.45) in G₃ mTERC^{-/-} mice.

Therefore, the low prevalence of SA β -galactosidase-positive cells in mTERC^{+/+} mice was independent of telomere shortening, possibly resembling the ‘premature senescence’ phenotype induced by mitogenic stimulation such as ras signaling (Serrano *et al.*, 1997). Although interference of SA β -galactosidase staining or senescence *per se* with telomere probe hybridization and measurement during qFISH remains formally possible, the data showing similar telomere fluorescence intensity in SA β -galactosidase-positive and -negative liver cells of mTERC^{+/+} mice indicate that such interference did not occur.

The Rb and p53 pathways have been prominently associated with cellular senescence (Bond *et al.*, 1996; Vaziri and Benchimol, 1996; Jarrard *et al.*, 1999; Bringold and Serrano, 2000; Smogorzewska and de Lange, 2002).

To test for activation of these senescence pathways in mTERC^{-/-} mice, Affimetrix oligonucleotide microarray analysis was carried out in duplicate comparing gene expression levels in quiescent liver and at the G₁/S transition (30–36 h after PH). This time point was chosen since most of the known senescence pathways are active at this transition point (Pang and Chen, 1994; Chen, 1997). We monitored gene expression changes between these two time points and compared the differentially regulated genes in mTERC^{+/+} and G₃ mTERC^{-/-} mice. This experiment identified 114 differentially expressed genes, 34 genes that were regulated in mTERC^{+/+} but not G₃ mTERC^{-/-} mice and 79 genes that were regulated in G₃ mTERC^{-/-} mice but not mTERC^{+/+} mice (data not shown). The full dataset of this microarray experiment is accessible

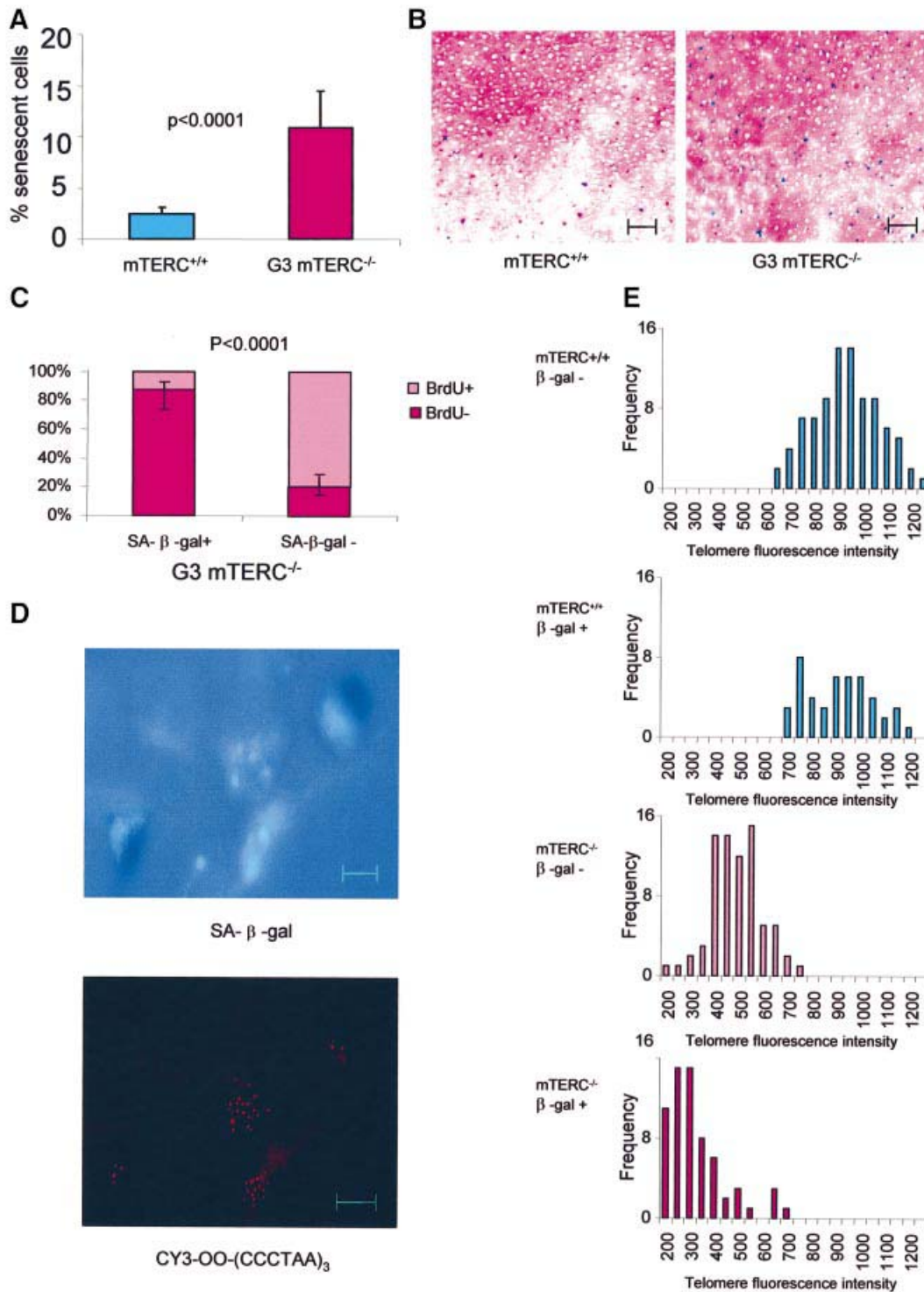


Fig. 3. Co-localization of SA β -galactosidase activity in non-proliferating cells with critically short telomeres. **(A)** SA β -galactosidase staining at pH 6 shows a higher number of positive cells in G₃ mTERC^{-/-} ($n = 5$) mice ($10.83 \pm 3.61\%$) compared with mTERC^{+/+} ($n = 5$) mice ($2.54 \pm 0.7\%$, $p < 0.0001$). **(B)** Representative photographs of SA β -galactosidase-stained liver sections (120 h after PH) of mTERC^{+/+} and G₃ mTERC^{-/-} mice (bar, 300 μ m). **(C)** Co-localization of SA β -galactosidase activity in non-proliferating liver cells of G₃ mTERC^{-/-} mice. Only $13 \pm 4.84\%$ of the SA β -galactosidase-positive cells are BrdU positive, whereas $79 \pm 6.2\%$ of the SA β -galactosidase-negative cells are BrdU positive. **(D)** Representative photograph of SA β -galactosidase and telomere probe co-staining showing that the fluorescent intensity of telomere spots is weaker in SA β -galactosidase-positive cells. **(E)** The frequencies of mean telomere fluorescence intensities in nuclei of (top to bottom) SA β -galactosidase-negative cells in mTERC^{+/+}, SA β -galactosidase-positive cells in mTERC^{+/+}, SA β -galactosidase-negative cells in G₃ mTERC^{-/-} and SA β -galactosidase-positive cells in mTERC^{-/-}. In total, the fluorescence intensities of telomere spots were analyzed from 89 SA β -galactosidase-negative cells (963.10 ± 130.65) and 46 SA β -galactosidase-positive cells (937.30 ± 135) from mTERC^{+/+} ($n = 5$) and from 75 SA β -galactosidase-negative cells (521.86 ± 100.16) and 65 SA β -galactosidase-positive cells (352.13 ± 119.63) from mTERC^{-/-} ($n = 5$) mice. Note that the telomere fluorescence intensity in mTERC^{+/+} mice is similar between SA β -galactosidase-positive and -negative cells, indicating that SA β -galactosidase staining did not interfere with telomere probe hybridization and measurement.

Table I. Differentially expressed cell cycle regulating genes at G₀-G₁/S transition in G₃ mTERC^{-/-} mice

No.	Gene description	Symbol	Δ RT-PCR	Function	Gene bank
1	Cyclin-dependent kinase inhibitor 1A, p21	<i>Cdkn1a</i>	6.02	Senescence, DNA damage response, cell cycle regulation	Aw048937
2	Fas associated factor 1	<i>Faf1</i>	-4.08	Apoptosis	U39643
3	Growth arrest and DNA damage inducible	<i>Gadd45g</i>	5.09	DNA damage response, cell cycle arrest	Af055638
4	Krupple-like factor 4	<i>Klf4</i>	5.77	DNA damage response	U20344
5	Nucleobindin2	<i>Nucb2</i>	12.9	Cell cycle regulation, growth arrest	Aj222586
6	P ⁸⁷ Wee1 kinase	<i>Wee1</i>	-5.93	DNA damage response, cell cycle regulation	D30743
7	Polo-like kinase	<i>Plk</i>	8.63	DNA damage response, cell cycle regulation	Av305987
8	Protein kinase inhibitor p ⁵⁸	<i>Prkri</i>	3.60	Growth regulation	U28423

Δ is the fold change of gene expression.

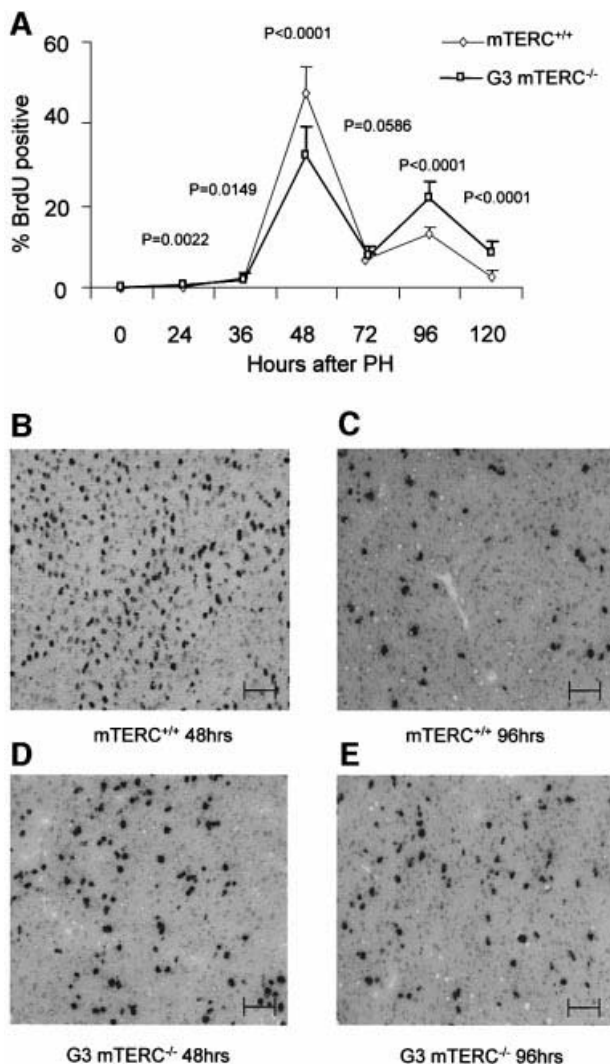


Fig. 4. Cells with sufficient telomere reserves compensate for impaired organ regeneration by an additional round of replication. (A) Percentage of BrdU-positive cells at different time points after PH in mTERC^{+/+} and G₃ mTERC^{-/-} mice as determined by 2 h of BrdU pulse labeling. (B-E) Representative photographs of the BrdU staining pattern at the two peak stages of S-phase in mTERC^{+/+} and G₃ mTERC^{-/-} mice (bar, 150 μm). mTERC^{+/+} mice show a higher percentage of BrdU-positive cells (47.03 ± 6.33%, n = 5) at the first-peak stage of S-phase (48 h after PH) compared with G₃ mTERC^{-/-} mice (32.31 ± 6.65%, n = 5, p < 0.0001). In contrast, at the second-peak stage of S-phase (96 h after PH), G₃ mTERC^{-/-} mice show a higher percentage of BrdU-positive cells (21.58 ± 4.24%, n = 5) compared with mTERC^{+/+} mice (12.66 ± 1.69%, n = 5, p < 0.0001).

in MIAME format online (www.gbf.de/array) under downloads (under Satyanarayana *et al.*: Table1, Table2 and ExperimentalDesign). From the differentially regulated genes in the microarray experiments comparing resting liver and regenerating liver 30–36 h after PH in mTERC^{+/+} mice and G₃ mTERC^{-/-} mice, eight target genes which have a role in cell cycle regulation were chosen and their differential expression was confirmed by RT-PCR (Table I). The gene list include four downstream targets of p53 (*p21*, *plk*, *Gadd45g* and *KLF-4*) which were all upregulated in G₃ mTERC^{-/-} mice; two of these genes (*p21* and *Gadd45g*) have previously been related to replicative senescence and DNA damage response that leads to G₁/S arrest (Dulic *et al.*, 2000; Vairapandi *et al.*, 2002).

To analyze the role of factors other than impaired cell cycle re-entry that could explain the decreased rate of proliferation in G₃ mTERC^{-/-} mice, we evaluated mitogenic signaling and apoptosis in this system. The most prominent mitogenic signal priming liver cells to re-enter the cell cycle is interleukin 6 (IL-6) (Cressman *et al.*, 1996; Li *et al.*, 2001). Induction and peak levels of IL-6 in response to PH were similar in mTERC^{+/+} and G₃ mTERC^{-/-} mice (data not shown), indicating that impaired mitogen responses did not account for the defective liver regeneration in G₃ mTERC^{-/-} mice. Apoptosis has been linked to impaired organ regeneration of highly self-renewing organs in mTERC^{-/-} mice (Lee *et al.*, 1998) and is induced by telomere shortening in clonally regenerating hepatocytes in the setting of acute liver failure (Rudolph *et al.*, 2000). We assessed the possible impact of apoptosis in our experimental system using the TUNEL assay. Following PH, TUNEL staining showed very low but similar rates of apoptosis in the liver of mTERC^{+/+} and G₃ mTERC^{-/-} mice (data not shown), suggesting that this process did not account for the differences in regenerative response. Given that apoptosis is predominantly present in the setting of telomere shortening coupled with extensive regenerative pressure in mTERC^{-/-} mice (Lee *et al.*, 1998; Rudolph *et al.*, 2000), it seems possible that the limited apoptotic response to PH was indicative of the more moderate regenerative stress in this setting.

Cells with sufficient telomere reserves in G₃ mTERC^{-/-} mice compensate for impaired organ regeneration by an additional round of replication
Synchronized liver regeneration in response to two-thirds PH takes approximately one and a half rounds of

replication to restore organ mass within a week after PH (Fausto, 2000; Kountouras *et al.*, 2001). In the C57BL/6 mouse strain used in our studies, the first peak stage of S-phase was observed 48 h after PH and was followed by a smaller second peak 96 h after PH (Figure 4). We evaluated S-phase onset and progression in response to PH in mTERC^{+/+} mice and G₃ mTERC^{-/-} mice by BrdU pulse labeling (Figure 4A). In response to PH, the timing of the

onset and the peak stages of S-phase were superimposable in mTERC^{+/+} and G₃ mTERC^{-/-} mice. Nevertheless, the percentage of liver cells participating in the first round of replication was significantly lower in G₃ mTERC^{-/-} mice than in mTERC^{+/+} mice (Figure 4A, B and D). In contrast, a significantly higher fraction of liver cells entered a second round of replication in G₃ mTERC^{-/-} mice than in mTERC^{+/+} mice (Figure 4A, C and E).

To test whether impaired S-phase entry would impact on organ regeneration and whether the elevated second round of replication could compensate for impaired regeneration, we followed the relative liver weight (liver weight/total body weight) of mTERC^{+/+} and G₃ mTERC^{-/-} mice at different time points after PH. In parallel with the time course of S-phase, the liver weight of G₃ mTERC^{-/-} mice compared with mTERC^{+/+} mice was significantly decreased after the first round of replication, 72 h after PH (relative liver weight 2.27% in G₃ mTERC^{-/-} mice compared with 2.74% in mTERC^{+/+} mice, $p = 0.001$). In agreement with our hypothesis that liver cells with sufficient telomere reserves accomplished organ regeneration in G₃ mTERC^{-/-} mice by entering a second round of replication, the liver weight was normalized in G₃ mTERC^{-/-} mice after the second round of replication, 120 h after PH (data not shown). Similarly, the difference in total number of BrdU-labeled cells (after long-term labeling) between G₃ mTERC^{-/-} and mTERC^{+/+} mice (Figure 1A and B) was significantly reduced after the second round of replication compared with the first round (-4.69% , $p = 0.0274$).

Together, our data indicated that impaired liver regeneration was due to inhibition of cell cycle re-entry in a subpopulation of cells with critically short telomeres in G₃ mTERC^{-/-} mice but was compensated for by an additional round of replication by liver cells with sufficient telomere reserves capable of proliferation. An alternative explanation was that a subpopulation of resting liver cells in G₃ mTERC^{-/-} mice was not in the G₀ stage but was arrested in G₂/M, and was released from this block to exit mitosis and therefore re-entered the cell cycle at a delayed time point after PH. To test this possibility, cell cycle analysis was carried out by flow cytometry on resting and regenerating livers of mTERC^{+/+} and G₃ mTERC^{-/-} mice (Figure 5). Since in mouse liver a relatively high percentage of cells are binucleated, this analysis was carried out on cell nuclei, although cytopspins on liver cells did not show a difference in the percentage of mononuclear (22.51 ± 7.77 versus 25.66 ± 3.83 , $p = 0.2645$) as well as binucleated (76.99 ± 8.90 versus 74.32 ± 3.82 , $p = 0.395$) cells in mTERC^{+/+} and G₃ mTERC^{-/-} mice. In line with previous reports of flow cytometry on liver cell nuclei of several strains of mice (Severin *et al.*, 1984; Danielsen *et al.*, 1986), our study revealed that in addition to a cell population with a 2N DNA content, a proportion of resting liver cell nuclei had a 4N DNA content. Cell cycle analysis of resting liver cell nuclei from G₃ mTERC^{-/-} and mTERC^{+/+} mice revealed a similar distribution of nuclei with 2N and 4N DNA content in both groups (Table II; Figure 5A and B). In line with the BrdU staining data, the FACS analysis revealed that 48 h after PH the overall number of cells in S-phase was significantly lower in G₃ mTERC^{-/-} than in mTERC^{+/+} mice (Table II; Figure 5C and D, top panel). Interestingly, the suppression of S-phase

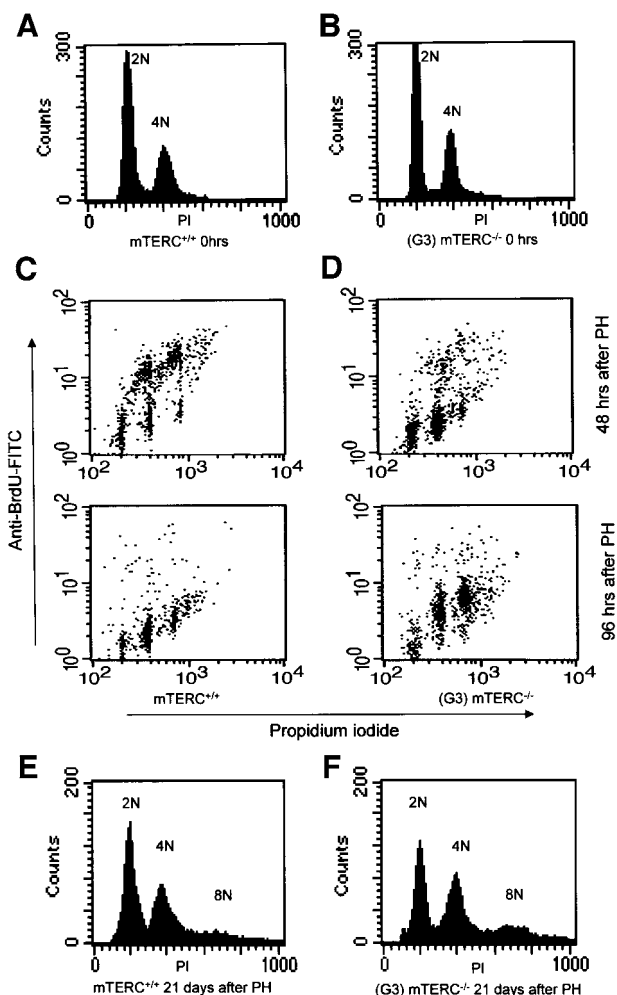


Fig. 5. Inhibition of S-phase entry, impaired G₂/M progression and an additional round of cell division in regenerating liver of G₃ mTERC^{-/-} mice. (A–F) Representative photographs of one of the five independent flow cytometric analyses of liver nuclei at each time point from mTERC^{+/+} and G₃ mTERC^{-/-} mice. (A and B) Ploidy distribution of cell nuclei from quiescent liver showing an almost similar composition of 2N and 4N nuclei in mTERC^{+/+} and G₃ mTERC^{-/-} mice. (C and D) Cell cycle profile of liver nuclei 48 h after PH (top panel) shows that a significantly lower number of 2N ($p = 0.0031$) and 4N ($p = 0.0219$) nuclei are positive for BrdU in G₃ mTERC^{-/-} than in mTERC^{+/+} mice, indicating that G₁/S progression was inhibited in a subset of liver cells in G₃ mTERC^{-/-} mice. In contrast, an increased number of 2N ($p = 0.0516$), 4N ($p = 0.0005$) and 8N ($p = 0.0074$) nuclei incorporate BrdU at 96 h (lower panel) after PH in G₃ mTERC^{-/-} than in mTERC^{+/+} mice, indicating that a higher number of liver cells in G₃ mTERC^{-/-} mice entered a second round of replication. Besides this difference in BrdU incorporation, there is an accumulation of cells with higher DNA content in G₃ mTERC^{-/-} mice during the time course of liver regeneration, indicating that G₂/M progression was impaired. (E and F) Ploidy distribution of liver nuclei 21 days after PH again showing an almost similar DNA content in mTERC^{+/+} and mTERC^{-/-} 2N ($p = 0.0683$), 4N ($p = 0.9831$) and 8N ($p = 0.0641$), indicating partial rescue of G₂/M arrest in the course of time.

Table II. Ploidy distribution and cell cycle profile of quiescent and proliferating liver cells at the indicated time points after PH in mTERC^{+/+} and G₃ mTERC^{-/-} as analyzed by flow cytometry

Time	2N	4N	8N	2N S-phase	4N S-phase	8N S-phase
mTERC ^{+/+} 0 h	62.37 ± 6.06	37.6 ± 6.03	–	–	–	–
G ₃ mTERC ^{-/-} 0 h	58.94 ± 4.88	41.09 ± 4.93	–	–	–	–
mTERC ^{+/+} 48 h after PH	22.15 ± 11.34	26.75 ± 7.53	9.62 ± 3.3	11.93 ± 5.73	21.3 ± 10.6	8.15 ± 3.33
G ₃ mTERC ^{-/-} 48 h after PH	23.42 ± 9.26	44.76 ± 11.12	17 ± 7.31	1.76 ± 0.84	8.15 ± 1.47	4.73 ± 1.34
mTERC ^{+/+} 96 h after PH	43.18 ± 17.25	40.87 ± 13.46	10.98 ± 7.77	1.58 ± 0.83	1.49 ± 1.13	1.36 ± 1.13
G ₃ mTERC ^{-/-} 96 h after PH	20.14 ± 6.42	43.26 ± 8.68	25.46 ± 9.86	2.84 ± 1.02	4.41 ± 0.62	4.05 ± 1.29
mTERC ^{+/+} 21 days after PH	49.93 ± 2.64	42.97 ± 2.79	6.24 ± 1.33	–	–	–
G ₃ mTERC ^{-/-} 21 days after PH	42.89 ± 0.72	42.92 ± 1.68	14.43 ± 2.77	–	–	–

entry in G₃ mTERC^{-/-} mice affected cells with 2N, 4N and higher DNA content. Although it cannot be excluded that some of the 4N and 8N cells were arrested at the G₂/M stage of the cell cycle, the inhibition of S-phase entry from 2N cells indicated that suppressed S-phase entry in G₃ mTERC^{-/-} was at least in part due to a pre-S-phase arrest.

As anticipated from the BrdU staining results (Figure 4), FACS analysis at 96 h after PH revealed a higher percentage of liver cells in S-phase in G₃ mTERC^{-/-} than in mTERC^{+/+} mice (Table II; Figure 5C and D, bottom panel). The fact that this S-phase entry predominantly derived from cells with 4N and 8N DNA content suggested that the second peak of S-phase in G₃ mTERC^{-/-} mice did not result from 4N cells overcoming a G₂/M block to re-enter S-phase from a 2N stage after completion of mitosis.

In addition to the above data on S-phase entry, the FACS analysis revealed an accumulation of cells with higher DNA content in G₃ mTERC^{-/-} compared with mTERC^{+/+} mice in the time course of liver regeneration following PH. These data are in line with previous reports of an impaired G₂/M progression of regenerating liver cells in mTERC^{-/-} mice (Rudolph *et al.*, 2000). Cell cycle analysis 21 days after PH again revealed an almost similar ploidy distribution in mTERC^{+/+} and G₃ mTERC^{-/-} mice (Figure 5E and F), indicating that impaired G₂/M progression in G₃ mTERC^{-/-} was either temporary or associated with decreased cell survival over time.

Discussion

Our current study demonstrates that telomere shortening at the cellular level affects organ regeneration *in vivo* by inhibiting a subpopulation of cells with critically short telomeres from entering the cell cycle, thereby limiting the pool of proliferating cells within an organ system. As a result, there is an elevated regenerative pressure on the proliferating subpopulation of cells to compensate for impaired organ regeneration by additional rounds of cell division, which in turn accelerates the rate of telomere shortening and the imbalance of proliferating and non-proliferating cells. Our results are further strengthened by previous studies in mTERC^{-/-} mice showing that it is not the average telomere length but the prevalence of critically short telomeres that leads to regenerative disorders (Hemann *et al.*, 2001). The new concept derived from our study is that the prevalence of critically short telomeres at the cellular level determines the proliferative capacity of cells within an organ system. Thus, the regenerative capacity of organs and tissues depends on the

size of the population of cells with sufficient telomere reserves required for cell proliferation.

Which mechanism limits cell proliferation in the subpopulation of cells with critically short telomeres? We show that mitogen signaling and apoptosis do not contribute to impaired liver regeneration in response to telomere shortening in our model system of PH. It seems likely that the lack of telomere-directed apoptosis reflects the modest regenerative stress induced by PH since we have previously shown that critical telomere shortening induces prominent hepatocyte apoptosis during clonal expansion of hepatocytes following acute liver failure—a setting of potent regenerative stress. The prevalence of β-galactosidase-positive cells and the coincidence of β-galactosidase activity with non-proliferating cells indicate that the cells with critically short telomeres have reached the senescence stage. In line with this hypothesis, gene expression profiling and RT-PCR analysis of regenerating liver at the onset of S-phase revealed an upregulation of downstream targets of p53 (Table I)—a pathway critical for inducing cellular senescence in response to telomere shortening (Vaziri and Benchimol, 1996; Chin *et al.*, 1999; Smogorzewska and de Lange, 2002).

At which stage of the cell cycle are the liver cells arrested? Previous studies in mTERC^{-/-} mice have revealed that telomere shortening induces a biphasic cell cycle block in mouse embryonic fibroblasts (Chin *et al.*, 1999) and impaired mitotic progression in regenerating liver (Rudolph *et al.*, 2000). In line with these studies, our current data on liver regeneration following PH show impaired cell cycle progression at two stages: pre-S-phase and G₂/M. Impaired S-phase entry in G₃ mTERC^{-/-} mice was independent of the DNA content of the cells, demonstrating that G₁/S progression was impaired, and the accumulation of cells with higher DNA ploidy in G₃ mTERC^{-/-} mice during the time course of liver regeneration indicated that G₂/M progression was impaired. We hypothesize that if telomeres are dysfunctional in resting cells, cell cycle re-entry is inhibited at the G₁/S transition. In addition, some cells will acquire dysfunctional telomeres during S-phase owing to further telomere shortening during DNA replication and will consequently be withdrawn from the cell cycle at the G₂/M stage.

Our study supports a model in which inhibition of cell cycle entry in a subpopulation of cells with critically short telomeres results in delayed organ regeneration by requiring an additional round of replication by cells with sufficient telomere reserves. According to this model,

regenerative defects are determined by the size of the proliferating population of cells within an organ system necessary to maintain organ function and homeostasis. It seems likely that the differences in telomere length between individual cells within an organ reflect the replicative history of cells during organogenesis and postnatal life. In addition, other factors that possibly affect telomere length might be differences in metabolic rates and intracellular load of radical oxygen species. The percentage of liver cells inhibited from cell cycle re-entry in G_3 mTERC^{-/-} mice in our study was ~15%; most of them (~11%) in turn show β -galactosidase activity. The mice do not show any liver phenotype during development and aging, but show an accelerated onset of cirrhosis in response to chronic organ damage (S.U. Wiemann and K.L. Rudolph, unpublished data) similar to the results obtained from G_6 mTERC^{-/-} mice in a mixed genetic background (Rudolph *et al.*, 2000). Therefore, the relatively small percentage of senescent cells inhibited from cell cycle re-entry seems to allow normal organ homeostasis in normal conditions, but under circumstances of elevated cell turnover it leads to impaired organ homeostasis.

Does the telomere hypothesis of impaired organ regeneration in mouse models apply to humans? To date there is an accumulation of correlative data indicating that telomere shortening might impact on the regenerative capacity of human tissues during aging and chronic diseases. In addition, mutation of the essential RNA component of human telomerase has been implicated in premature aging, bone marrow failure and liver cirrhosis among other phenotypes in patients with dyskeratosis congenita (Vulliamy *et al.*, 2001). Interestingly, in human cirrhosis, the prevalence of senescent hepatocytes ranges from 2 to 15% in the vast majority of cases, indicating that cellular senescence at rates similar to those observed in our study impairs regular organ regeneration in chronic liver disease in humans (Wiemann *et al.*, 2002). Determination of the rates of cellular senescence and the identification of new markers of senescence could be useful to test the relevance of senescence in limiting the regenerative capacity in different human tissues and organs during aging and chronic disease.

Materials and methods

Mice

Male mTERC^{-/-} and littermate mTERC^{+/+} control mice (age 10–12 weeks) in a C57/B6J background were used for this study. The mice were bred and maintained in the animal facility, Medical School Hannover, Germany, on a standard diet.

Partial hepatectomy and BrdU labeling

All the mice were operated on in the morning (between 8.00 and 11.00 a.m.) as described (Higgins and Anderson, 1931). Mice were anesthetized and subjected to 70% PH by surgically removing the left lateral, left median and right median lobes without disrupting the portal vein, biliary tract and gallbladder. The mice were killed from each group (mTERC^{+/+} and mTERC^{-/-}) at 24 h ($n = 3$), 36 h ($n = 3$), 48 h ($n = 5$), 72 h ($n = 5$), 96 h ($n = 5$) and 120 h ($n = 5$) after PH. Ten microliters per gram body weight of labeling reagent [10:1 ratio, BrdU and 5-fluoro-20-deoxyuridine (Cell Proliferation Kit, Amersham)] were administered to the animals intraperitoneally 2 h before killing. For continuous labeling of all the proliferating cells, 0.8 mg/ml BrdU (Sigma) was given in sterile drinking water and fresh water was prepared every 24 h. To increase the sensitivity of the continuous labeling procedure, 200 μ l of 1 mg/ml BrdU

in phosphate-buffered saline (PBS) were administered intraperitoneally at 12 h intervals between 24 and 72 h (or 120 h) after PH. After killing, the liver lobes were snap frozen in liquid nitrogen and stored at -80°C until required for further analysis.

Immunohistochemical detection of BrdU

After fixation of 7 μ m cryostat sections in ice-cold acetone–methanol (1:1) for 10 min, samples were washed in Tris-buffered saline (TBS)–Tween, dehydrated in 70% ethanol for 30 min and air dried. Endogenous peroxidase activity was blocked by 3% H_2O_2 in methanol for 10 min, followed by two 5 min washes in TBS–Tween, denaturation in alkaline formamide (95 ml formamide + 5 ml 1N NaOH) for 30 s at 70°C , washing for 5 min in TBS–Tween at 70°C and incubation in 15 mM tri-sodium citrate in formamide for 15 min at 70°C . The reaction was stopped by washing the slides in ice-cold TBS–Tween twice for 5 min each. A second fixation was carried out in 3% formaldehyde in PBS for 30 min, followed by two 5 min washes in TBS–Tween and incubation in 0.2% glutaraldehyde in PBS for 10 min at room temperature. The slides were then washed twice for 5 min in TBS–Tween and incubated with anti-BrdU monoclonal antibody overnight at 4°C in a wet chamber. After two washes with TBS–Tween, the slides were incubated with a peroxidase-labeled anti-mouse IgG2a secondary antibody for 30 min at room temperature, followed by three 5 min washes, and detection was performed by incubating them with the substrate 3,3'-diaminobenzidine tetrahydrochloride (DAB) (25 mg of DAB, 100 μ l of substrate intensifier, 50 ml of PBS) for 20 min, followed by two 5 min washes with double-distilled water. The slides were then counterstained with hemalum solution, mounted with mounting medium and stored in the dark until analysis. A BrdU-labeling index was determined by counting the number of BrdU-positive cells randomly in 20 low-power magnification fields ($10\times$) and expressing the number of BrdU-labeled nuclei as a percentage of all nuclei counted.

Senescence-associated β -galactosidase staining

Senescence-associated β -galactosidase staining was carried out as described previously (Dimri *et al.*, 1995). All the samples were stained in triplicate. Analysis was carried out in blinded fashion. The number of SA β -galactosidase-positive cells was counted randomly in 20 low-power fields ($10\times$) and expressed as a percentage of all cells counted.

BrdU–telomere probe co-staining

Cryostat sections (7 μ m) were fixed, dehydrated and denatured exactly as described above. Following the second fixation in 3% formaldehyde in PBS, the tissues were digested with acidified pepsin (100 mg of pepsin, 100 ml of H_2O , 84 μ l of conc. HCl) for 10 min, followed by two 5 min washes in TBS–Tween. Then they were fixed by incubating in 0.2% glutaraldehyde in PBS for 10 min at room temperature. The slides were co-incubated with anti-BrdU monoclonal antibody (Amersham) and telomere probe hybridization mix [250 μ l final volume: 2.5 μ l of 1 M Tris–HCl pH 7.2, 21.4 μ l of MgCl_2 (25 mM MgCl_2 , 9 mM citric acid, 82 mM Na_2HPO_4 pH 7.4), 175 μ l of deionized formamide, 12.5 μ l of 10% (w/w) blocking reagent, 5 μ l of 25 $\mu\text{g}/\text{ml}$ PNA Cy3-telomere probe, 33.6 μ l of H_2O] overnight at 4°C in a wet chamber. Then they were given three 5 min washes with TBS–Tween and incubated with FITC-conjugated goat anti-mouse IgG secondary antibody (Dako) for 30 min at room temperature, followed by three 5 min washes in TBS–Tween and mounting in DAPI mounting solution. The telomere fluorescence intensities were calibrated as described (Herrera *et al.*, 1999; Wiemann *et al.*, 2002). Quantification of the telomere fluorescence intensity was performed on cy3 and DAPI images captured at a magnification of $100\times$ using TFL-TELO V1.0, a telomere analysis program developed by P.Landsdorp.

Senescence–BrdU co-staining

For simultaneous detection of senescence and cell proliferation in the same sample, first SA β -galactosidase staining at pH 6 was carried out (as described above) on 7 μ m sections of liver samples from mTERC^{+/+} ($n = 5$) and mTERC^{-/-} ($n = 5$), followed by BrdU staining as described above.

Senescence–telomere probe co-staining

To measure the telomere lengths in senescent cells and proliferating cells in the same sample, first SA β galactosidase staining was carried out (as described above), followed by telomere probe hybridization (as described above), except that the pepsin digestion step was optimized to 7 min to detect cytoplasmic senescent staining and at the same time to minimize background for telomere fluorescence intensity measurement.

Apoptosis staining

The tunnel assay was performed on cryostat sections according to the manufacturer's protocol (In Situ Cell Death Detection Kit, Roche). The number of apoptotic cells was counted in 20 high-power fields (100×). All the counts were performed without knowledge of the day(s) after PH.

Determination of IL-6 serum levels

Sera were obtained from partially hepatectomized mice at 1, 3, 6, 9 and 12 h, and stored at -80°C before testing. Serum IL-6 levels were determined using the Pharmingen OptEIA™ Set: Mouse IL-6 kit according to the manufacturer's protocol.

Liver perfusion, nuclei preparation and flow cytometry

Liver cells were collected by the collagenase perfusion method. The cells were collected from the quiescent liver (non-operated) ($n = 5$) and 48 h ($n = 6$), 96 h ($n = 5$) and 21 days ($n = 4$) after PH from each group (mTERC^{+/+} and mTERC^{-/-}). Mice were anesthetized and subjected to 70% PH, and 10 µl/g body weight labeling reagent [10:1 ratio of 5-BrdU and 5-fluoro-20-deoxyuridine (Cell Proliferation Kit, Amersham)] was administered 2 h before liver perfusion. The liver was perfused through the portal vein by inserting a SURFLO I.V catheter connected to an ISMATEC pump with KRBI buffer (150 mM NaCl, 5 mM KCl, 5 mM glucose, 25 mM NaHCO₃, 20 mM HEPES, 1 mM EDTA pH 7.4 at 37°C) until the blood was completely drained out, followed by KRBII (150 mM NaCl, 5 mM KCl, 5 mM glucose, 25 mM NaHCO₃, 20 mM HEPES, 0.5 mM CaCl₂, 0.5 mg/ml collagenase at 37°C) until the liver mass became soft and fragile. The liver mass was suspended in 10 ml of PBS by gentle pipetting and then centrifuged at 50 g for 3 min for hepatocyte purification.

Next, 1×10^6 cells were suspended gently for 2 min without producing air bubbles in 2 ml of NPBT buffer (10 mM Tris-HCl pH 7.4, 2 mM MgCl₂, 140 mM NaCl, 0.5% Triton X-100) and centrifuged through a 50% sucrose gradient (50% sucrose in NPB, 10 mM Tris-HCl pH 7.4, 2 mM MgCl₂, 140 mM NaCl) for 10 min at 13 000 r.p.m. The nuclear pellet was resuspended in a suitable volume of PBS and again centrifuged at 50 g for 2 min to remove non-lysed cells. The pure nuclei obtained from this procedure were used for flow cytometry. The nuclei collected 0 h and 21 days after PH were stained with PI only, whereas the nuclei collected 48 and 96 h after PH were double stained with PI and FITC-antiBrdU antibody (Becton Dickinson) according to the manufacturer's instructions. Flow cytometric analysis was carried out with a FACScan (Becton Dickinson) equipped with Cellquest software.

RNA extraction and cDNA synthesis

The total RNA was extracted according to the manufacturer's protocol (RNA Clean™; Hybaid). The RNA extracted from the liver samples at 0 h [mTERC^{+/+} ($n = 6$), mTERC^{-/-} ($n = 5$)] and at 30–36 h after PH [mTERC^{+/+} ($n = 12$) and mTERC^{-/-} ($n = 10$)] and the RNA with an OD_{260/280} ratio of 2 or more was used for microarray, cDNA synthesis and quantitative real-time PCR. Two micrograms of total RNA were used to synthesize cDNA with oligo-dT primer and Superscript II-RT enzyme (Invitrogen). The RT reaction was checked by amplifying a 130 bp fragment of the housekeeping gene *RSP9*.

DNA microarray hybridization and analysis

The quality and integrity of the total RNA were checked by running all the samples on an Agilent Technologies 2100 Bioanalyzer (Agilent Technologies). The expression analysis was carried out according to the manufacturer's standard protocols (Affymetrix GeneChip Expression Analysis Manual; Affymetrix). A detailed description of the experimental set-up and the data analysis is accessible online (www.gbf.de/array) under downloads (under Satyanarayana *et al.*: ExperimentalDesign). The full dataset is accessible on the same web page under Table1 (full data set on signal intensities) and Table2 (conclusive data set on calculated gene expression changes).

Quantitative real-time PCR

Quantitative real-time PCR was performed on an ABI prism 7700 Sequence detection system (PE Applied Biosystems) using SYBR Green I as a double-strand DNA-specific binding dye. The same RNA preparations were used for microarray and quantitative RT-PCR. All the samples were analyzed in triplicate and the expression of each target gene was confirmed by three independent PCR runs. The cycle profile of PCR is as follows: an initial 10 min activation of Hot Star Taq™ DNA polymerase (Qiagen) at 95°C, followed by denaturation at 94°C for 15 s, annealing at 54°C for 15 s and extension at 72°C for 30 s. Forty cycles of PCR amplification were performed to confirm the expression levels of

eight selected target genes, and the housekeeping gene *RSP9* was used as an internal control to normalize the expression levels; the Ct for the target genes appears between 24 and 30 cycles. The quantification data were analyzed with the ABI Prism 7700 analysis software.

Statistical programs

Student's *t*-test, Fisher's exact test and Graphpad InStat software were used to calculate the statistical significance and standard deviations.

Acknowledgements

This paper is dedicated to the memory of Jo Lauber. We thank Professor Ungewickell for the fluorescence microscopy, and Dr R.Greenberg and Dr H.Sundberg for critical reading of the manuscript. K.L.R. is supported by grants from the Deutsche Forschungsgemeinschaft (Ru 745/2-1) and Deutsche Krebshilfe e.V. (10-1809-Ru1), M.A.B. is supported by grants from the Spanish Ministry of Science and Technology, the European Union and the Department of Immunology and Oncology (CSIC-Pharmacia Corporation).

References

- Allsopp,R.C. and Harley,C.B. (1995) Evidence for a critical telomere length in senescent human fibroblasts. *Exp. Cell Res.*, **219**, 130–136.
- Allsopp,R.C., Chang,E., Kashefi-Aazam,M., Rogaev,E.I., Piatyszek,M.A., Shay,J.W. and Harley,C.B. (1995) Telomere shortening is associated with cell division *in vitro* and *in vivo*. *Exp. Cell Res.*, **220**, 194–200.
- Ball,S.E., Gibson,F.M., Rizzo,S., Tooze,J.A., Marsh,J.C. and Gordon-Smith,E.C. (1998) Progressive telomere shortening in aplastic anemia. *Blood*, **91**, 3582–3592.
- Blackburn,E.H. (1991) Structure and function of telomeres. *Nature*, **350**, 569–573.
- Blasco,M.A., Lee,H.W., Hande,M.P., Samper,E., Lansdorff,P.M., DePinho,R.A. and Greider,C.W. (1997) Telomere shortening and tumor formation by mouse cells lacking telomerase RNA. *Cell*, **91**, 25–34.
- Bodnar,A.G. *et al.* (1998) Extension of life-span by introduction of telomerase into normal human cells. *Science*, **279**, 349–352.
- Bond,J., Houghton,M., Blydes,J., Gire,V., Wynford-Thomas,D. and Wyllie,F. (1996) Evidence that transcriptional activation by p53 plays a direct role in the induction of cellular senescence. *Oncogene*, **13**, 2097–2104.
- Boulwood,J., Peniket,A., Watkins,F., Shepherd,P., McGale,P., Richards,S., Fidler,C., Littlewood,T.J. and Wainscoat,J.S. (2000) Telomere length shortening in chronic myelogenous leukemia is associated with reduced time to accelerated phase. *Blood*, **96**, 358–361.
- Bringold,F. and Serrano,M. (2000) Tumor suppressors and oncogenes in cellular senescence. *Exp. Gerontol.*, **35**, 317–329.
- Chang,E. and Harley,C.B. (1995) Telomere length and replicative aging in human vascular tissues. *Proc. Natl Acad. Sci. USA*, **92**, 11190–11194.
- Chen,K.Y. (1997) Transcription factors and the down-regulation of G₁/S boundary genes in human diploid fibroblasts during senescence. *Front. Biosci.*, **2**, 417–426.
- Chin,L., Artandi,S.E., Shen,Q., Tam,A., Lee,S.L., Gottlieb,G.J., Greider,C.W. and DePinho,R.A. (1999) p53 deficiency rescues the adverse effects of telomere loss and cooperates with telomere dysfunction to accelerate carcinogenesis. *Cell*, **97**, 527–538.
- Cressman,D.E., Greenbaum,L.E., DeAngelis,R.A., Ciliberto,G., Furth,E.E., Poli,V. and Taub,R. (1996) Liver failure and defective hepatocyte regeneration in interleukin-6 deficient mice. *Science*, **274**, 1379–1383.
- Danielsen,H., Lindmo,T. and Reith,A. (1986) A method for determining ploidy distributions in liver tissue by stereological analysis of nuclear size calibrated by flow cytometric DNA analysis. *Cytometry*, **7**, 475–480.
- Dimri,G.P. *et al.* (1995) A biomarker that identifies senescent human cells in culture and in aging skin *in vivo*. *Proc. Natl Acad. Sci. USA*, **92**, 9363–9367.
- Dulic,V., Beney,G.E., Frebourg,G., Drullinger,L.F. and Stein,G.H. (2000) Uncoupling between phenotypic senescence and cell cycle arrest in aging p21-deficient fibroblasts. *Mol. Cell. Biol.*, **20**, 6741–6754.

- Effros,R.B. (2000) Telomeres and HIV disease. *Microbes Infect.*, **2**, 69–76.
- Fausto,N. (2000) Liver regeneration. *J. Hepatol.*, **32**, 19–31.
- Gonzalez-Suarez,E., Samper,E., Flores,J.M. and Blasco,M.A. (2000) Telomerase-deficient mice with short telomeres are resistant to skin tumorigenesis. *Nat. Genet.*, **26**, 114–117.
- Harley,C.B., Futcher,A.B. and Greider,C.W. (1990) Telomeres shorten during ageing of human fibroblasts. *Nature*, **345**, 458–460.
- Hemann,M.T., Strong,M.A., Hao,L.Y. and Greider,C.W. (2001) The shortest telomere, not average telomere length, is critical for cell viability and chromosome stability. *Cell*, **107**, 67–77.
- Herrera,E., Samper,E., Martin-Caballero,J., Flores,J.M., Lee,H.W. and Blasco,M.A. (1999) Disease states associated with telomerase deficiency appear earlier in mice with short telomeres. *EMBO J.*, **18**, 2950–2960.
- Higgins,G.M. and Anderson,R.M. (1931) Experimental pathology of the liver. I. Restoration of the liver of the white rat following partial surgical removal. *Arch. Pathol.*, **12**, 186–202.
- Jarrard,D.F. *et al.* (1999) p16/pRb pathway alterations are required for bypassing senescence in human prostate epithelial cells. *Cancer Res.*, **59**, 2957–2964.
- Kinouchi,Y., Hiwatashi,N., Chida,M., Nagashima,F., Takagi,S., Maekawa,H. and Toyota,T. (1998) Telomere shortening in the colonic mucosa of patients with ulcerative colitis. *J. Gastroenterol.*, **33**, 343–348.
- Kitada,T., Seki,S., Kawakita,N., Kuroki,T. and Monna,T. (1995) Telomere shortening in chronic liver diseases. *Biochem. Biophys. Res. Commun.*, **211**, 33–39.
- Kountouras,J., Boura,P., Lygidakis,N.J. (2001) Liver regeneration after hepatectomy. *Hepatogastroenterology*, **48**, 556–562.
- Lee,H.W., Blasco,M.A., Gottlieb,G.J., Horner,J.W., 2nd, Greider,C.W. and DePinho,R.A. (1998) Essential role of mouse telomerase in highly proliferative organs. *Nature*, **392**, 569–574.
- Li,W., Liang,X., Leu,J.I., Kovalovich,K., Ciliberto,G. and Taub,R. (2001) Global changes in interleukin-6-dependent gene expression patterns in mouse livers after partial hepatectomy. *Hepatology*, **33**, 1377–1386.
- Lindsey,J., McGill,N.I., Lindsey,L.A., Green,DK. and Cooke,H.J. (1991) *In vivo* loss of telomeric repeats with age in humans. *Mutat. Res.*, **256**, 45–48.
- Pang,J.H. and Chen,K.Y. (1994) Global change of gene expression at late G₁/S boundary may occur in human IMR-90 diploid fibroblasts during senescence. *J. Cell. Physiol.*, **160**, 531–538.
- Paradis,V., Youssef,N., Dargere,D., Ba,N., Bonvoust,F., Deschatrette,J. and Bedossa,P. (2001) Replicative senescence in normal liver, chronic hepatitis C and hepatocellular carcinomas. *Hum. Pathol.*, **32**, 327–332.
- Poon,S.S. and Lansdorp,P.M. (2001) *Current Protocols in Cell Biology*. Wiley, New York, NY, pp. 18.4.1–18.4.21.
- Rudolph,K.L., Chang,S., Lee,H.-W., Blasco,M., Gottlieb,G.J., Greider,C. and DePinho,R.A. (1999) Longevity, stress response and cancer in aging telomerase deficient mice. *Cell*, **96**, 701–712.
- Rudolph,K.L., Chang,S., Millard,M., Schreiber-Agus,N. and DePinho,R.A. (2000) Inhibition of experimental liver cirrhosis in mice by telomerase gene delivery. *Science*, **287**, 1253–1258.
- Samper,E., Flores,J.M. and Blasco M.A. (2001) Restoration of telomerase activity rescues chromosomal instability and premature aging in *Terc*^{-/-} mice with short telomeres. *EMBO Rep.*, **2**, 800–807.
- Serrano,M., Lin,A.W., McCurrach,M.E., Beach,D. and Lowe,S.W. (1997) Oncogenic ras provokes premature cell senescence associated with accumulation of p53 and p16INK4a. *Cell*, **88**, 593–602.
- Severin,E., Willers,R. and Bettecken,T. (1984) Flow cytometric analysis of mouse hepatocyte ploidy. II. The development of polyploidy pattern in four mice strains with different life spans. *Cell Tissue Res.*, **238**, 649–652.
- Severino,J., Allen,R.G., Balin,S., Balin,A. and Cristofalo,V.J. (2000) Is β -galactosidase staining a marker of senescence *in vitro* and *in vivo*? *Exp. Cell Res.*, **257**, 162–171.
- Shay,J.W., Pereira-Smith,O.M. and Wright,W.E. (1991) A role for both RB and p53 in the regulation of human cellular senescence. *Exp. Cell Res.*, **196**, 33–39.
- Smogorzewska,A. and de Lange,T (2002) Different telomere damage signaling pathways in human and mouse cells. *EMBO J.*, **21**, 4338–4348.
- Vairapandi,M., Balliet,A.G., Hoffman,B. and Liebermann,D.A. (2002) GADD45b and GADD45g are cdc2/cyclinB1 kinase inhibitors with a role in S and G₂/M cell cycle checkpoints induced by genotoxic stress. *J. Cell. Physiol.*, **192**, 327–338.
- Vaziri,H. and Benchimol,S. (1996) From telomere loss to p53 induction and activation of a DNA-damage pathway at senescence: the telomere loss/DNA damage model of cell aging. *Exp. Gerontol.*, **31**, 295–301.
- Vaziri,H., Schachter,F., Uchida,I., Wei,L., Zhu,X., Effros,R., Cohen,D. and Harley,C.B. (1993) Loss of telomeric DNA during aging of normal and trisomy 21 human lymphocytes. *Am. J. Hum. Genet.*, **52**, 661–667.
- Vaziri,H., Dragowska,W., Allsopp,R.C., Thomas,T.E., Harley,C.B. and Lansdorp,P.M. (1994) Evidence for a mitotic clock in human hematopoietic stem cells: loss of telomeric DNA with age. *Proc. Natl Acad. Sci. USA*, **91**, 9857–9860.
- Vulliamy,T., Marrone,A., Goldman,F., Dearlove,A., Bessler,M., Mason,P.J. and Dokal,I. (2001) The RNA component of telomerase is mutated in autosomal dominant dyskeratosis congenita. *Nature*, **413**, 432–435.
- Wiemann,S.U. *et al.* (2002) Hepatocyte telomere shortening and senescence are general markers of human liver cirrhosis. *FASEB J.*, **16**, 935–942.
- Wright,W.E. and Shay,J.W. (1992) The two-stage mechanism controlling cellular senescence and immortalization. *Exp. Gerontol.*, **27**, 383–389.
- Yu,G.L., Bradley,J.D., Attardi,L.D. and Blackburn,E.H. (1990) *In vivo* alteration of telomere sequences and senescence caused by mutated *Tetrahymena* telomerase RNAs. *Nature*, **344**, 126–132.

Received September 2, 2002; revised May 21, 2003;
accepted June 2, 2003